This is an Accepted Manuscript of an article published by Taylor & Francis in Journal of the Operational Research Society on 8 February 2022, available at: https://doi.org/10.1080/01605682.2022.2035273
T. Jin, H. Li and S. P. Kumar Prabha, "Supply chain design for transactive energy operations in the nexus of manufacturing, microgrid and climate," Journal of the Operational Research Society, vol. 73, no. 11, pp. 2395-2411, 2022.

Supply Chain Design for Transactive Energy Operations in the Nexus of Manufacturing, Microgrid and Climate

Tongdan Jin[a]*, Honglin Li[b], Siva Prashanth Kumar Prabha[a]
[a]Industrial Engineering Program, Texas State University, San Marcos, TX 78666, USA
[b]Department of Mechanical Engineering, The University of Texas at Dallas, Richardson, TX 75080, USA
{*corresponding author, tj17@txstate.edu}

Abstract

Manufacturing and supply chain sectors are undergoing a paradigm change driven by the growing use of distributed renewable energy. Under demand and generation uncertainty, this paper aims to allocate wind turbine, solar photovoltaics and energy storage units in a three-tier supply chain network to achieve sustainable operations with minimum cost. We propose a mixed-integer stochastic programming model that involves the production-inventory and microgrid capacity decisions along with the hourly energy transactions to meet the electrical loads of factories, warehouse, and retail stores. Our study advances existing supply chain design methods by explicitly incorporating transactive energy, materials, information and cash flows into a holistic optimization framework. The performance and scalability of the model is tested in two network instances with various facility locations, machine capacity, and climate conditions. Results show that onsite renewable generation enables large industrial consumers to achieve environmental sustainability as well as to create new revenue stream through the participation in transactive energy market. The study also indicates that feed-in tariff, time-of-use rate, two-way energy trading can lower the utility cost and accelerate the adoption of variable generation technology.

Keywords: energy; inventory; production; supply chain; sustainability

1. Introduction

Manufacturing and supply chain industries are experiencing a paradigm change driven by carbon neuralization, logistics electrification, and distributed or microgrid generation (Martin 2012; Huddleston 2015; Parker et al. 2019). A microgrid system is formed by a group of local loads and distributed generation (DG) units that act as a single entity with respect to the main grid. Typical DG units include wind turbines (WT), photovoltaics (PV), biogas fuel cells, small hydro, combined heat and power, and energy storage system (ESS). In fact, a growing number of firms like Honda and Walmart are installing onsite WT and roof-top PV systems to energize their factories or commercial buildings for environmental sustainability (Stinpetru 2014, Ozment 2015). These renewables initiatives are re-shaping the business landscape by transforming the traditional firms from passive consumers to active energy prosumers (Progressive Grocer 2019; EIA 2019). An energy prosumer is referred to as an entity who consumes and produces electricity in a DG realm.

Transactive energy (TE) is defined as "a system of economic and control mechanisms that allows the dynamic balance of supply and demand across the entire electrical infrastructure using value as a key operational parameter" (DOE 2015). TE provides new functions and characteristics that allows for responsive load control, non-utility DG or microgrid integration, and end-use prosumer participation. Three types of TE operations have been discussed in literature: 1) coordinated operation that incorporates aggregation schemes for orchestrating a large number of DG or microgrids across power distribution network; 2) uncoordinated operation with self-interested prosumers and local energy management systems; and 3) peer-to-peer operation that considers decentralized energy trading between multiple prosumers (Guerrero et al. 2020). With the advent of blockchain technology, prosumer energy trading between microgrid and utility company is becoming technically feasible and financially viable by using distributed ledgers or

smart contracts (Tsao and Vu, 2021). This paper is focused on planning coordinated prosumer operations between a group of renewable microgrid systems and a large utility company. Particularly we aim at siting and sizing renewable microgrids in factories, warehouses and retail stores across a three-tier supply chain infrastructure. In addition to satisfying own energy needs, each facility behaves as an energy prosumer and engages TE trading through an aggregate market scheme.

Planning and operations of manufacturing supply chain has been the focal topic for decades in operations management community. The goal is to seek optimal procurement, production, and warehousing policy against various uncertainties, such as random yield (Yano and Lee 1995), product demand (Sox and Muckstadt 1996), machine capacity (Cheng et al. 2012), and lead time (Kok et al. 2018). For instance, Tan and Gershwin (2004) investigate a production-inventory system that involves one manufacturing firm and multiple subcontractors. A feedback policy that determines the firm's production quantity and supply rate of subcontractors is derived to jointly fulfil the volatile demands. Karen et al. (2004) propose a finite-state Markov decision model to optimize production and inventory level for minimizing an expected cost. They numerically solve the Hamilton-Jacobi-Bellman equations by considering random demand and process yield. Zhang et al. (2012) develop a polynomial-time dynamic programming algorithm to tackle a multi-echelon uncapacitated lot-sizing problem where the intermediate echelons face random demands externally and internally. Megahed and Goetschalckx (2018) design a multi-period, multi-echelon supply chain network that takes into account supplier's random yield, variable lead time and backorder penalty. Our paper also optimizes a multi-echelon production-inventory system considering product demand uncertainty, but the main focus is to allocate wind- and solar-based microgrids in geographically dispersed facilities to realize transactive energy operations.

This study contributes to the modeling and application of sustainable supply chain infrastructure in a distributed generation realm. In modeling, this paper takes an early step to incorporate prosumer microgrid generation in the design and operation of a three-tier supply chain network with two-way energy trading. Existing manufacturing supply chain models usually focus on the coordination of materials, information and cash flows, but microgrid integration coupled with transactive energy trading has not been adequately investigated. For applications, our work transforms the supply chain stakeholders from a passive energy consumer into an active electricity supplier through onsite wind and solar integration. This new feature enables factory operators, warehouse managers, and retailers to increase the value chain through logistics electrification, emissions reduction and socially-responsible production. The proposed model is able to address the requirements of environmental sustainability, energy independence, and prosumer economy through an integrated planning of production, inventory and renewables in the manufacturing-microgrid-climate nexus.

The remainder of the paper is organized as follows. Section 2 reviews the existing studies of designing low-carbon production-inventory systems. Section 3 presents an integrated production planning and microgrid sizing model with transactive energy trading in a three-tier supply chain setting. In Section 4, the hourly capacity factors of WT and PV for ten US cities are estimated based on 11-year hourly meteorological data. In Section 5, the integrated planning model is implemented in a two-factory, one-warehouse, and two-store network. Several managerial insights are also derived. In Section 6, an expanded supply chain comprised of ten facilities is used to demonstrate the model scalability. Section 7 concludes the paper.

2. Literature Review

Recently new production-inventory models have been developed to address carbon emissions and climate change issues. These studies can be classified into two categories: 1) market-driven emissions reduction and control mechanism; and 2) onsite renewable generation. Market-based mechanism include emission cap-and-trade policy (Pan et al. 2021), and tax intensive program (Drake et al. 2016). Emissions cap-and-trade has been implemented in North America, Europe, and other regions of the world. For instance, Gong and Zhou (2013) investigate a production-inventory system that can access a green and a regular production technology under emissions trading and allowances. The structural properties of the model are derived to characterize the optimal production policies and emissions trading for minimizing the expected total cost. Later, Zhang et al. (2016) extend the model to multi-technology systems with different emission rates. Similarly, Drake et al. (2016) study the impact of emissions tax, cap, and trade on a firm's technology choice and capacity decisions. They find that uncertain emissions price under cap-and-trade regulation leads to a greater profit margin than fixed price under an emissions tax. He et al. (2017) formulate a Stackelberg model to compare the optimal production planning of a manufacturer and the best cap setting of a regulator under the cap-and-trade regulation. Their study shows that the total emissions and the optimal cap increase initially and then decrease eventually as the emissions from one unit of product increases. Goodarzi et al. (2019) intend to identify the optimal feed-in tariff rate in a multi-player market involving grid operator, PV investor, and a trading regulator. Under the economic order quantity framework, Lee (2020) jointly determines the optimal order quantity and investment by comparing various cap-and-price policies, such as cap-and-trade, carbon tax, cap-and-offset, and carbon cap. The optimal solutions are characterized and compared in terms of the firm's annual total cost and carbon footprint. In summary, the essence

of these market-driven mechanisms is to motivate the firms to control and curb carbon and pollutant generation in exchange of financial benefits.

Onsite renewable generation differs from market-driven mechanism in that firms strive to achieve the environmental commitment by adopting and installing WT, PV, and other eco-friendly DG systems. Abdallah et al. (2013) present an economic model to calculate the levelized energy cost of a roof-top PV system deployed in supply chain facilities across 49 US states. A case study is used to demonstrate the product demand and weather dynamics that affect supplier selection, plant location and capacity, and PV sizing. Li et al. (2017) propose a zero-carbon energy supply model to guide the integration of onsite wind and solar generation into manufacturing and warehouse facilities. The goal is to minimize the levelized cost of renewable energy by sizing and siting WT, solar PV and energy storage units under stochastic weather condition. Golari et al. (2017) consider onsite and grid wind, solar and hydro power and integrate them in a multi-tier, production-inventory system to meet the green energy coefficient target. Subject to power intermittency, the optimal production policies and renewables supply are jointly coordinated in each period such that the total expected cost over the planning horizon is minimized. Pham et al. (2019) propose a two-stage production and renewable microgrid planning model to achieve net-zero energy operations in a disaggregate factory-warehouse setting. The first stage is to optimize the weekly production to meet the random customer demand over one-year period. The second stage allocates microgrid capacity, and schedule renewable power to balance the hourly energy needs. Our paper advances their work in two aspects. First, we formulate an integrated planning model where production, microgrid capacity, ESS operations, and TE trading are concurrently optimized in a three-tier supply chain setting. This ensures the global optimality compared with the two-stage or sequential decision. Second, transactive energy is explicitly considered as a new

decision variable and incorporated into the production-inventory model. Hence the new model represents a first-of-its-kind in synthesizing the commodity and the electricity markets under an aggregate energy trading mechanism between supply chain entities and utility grid.

3. Joint Production Planning and Microgrid Sizing

3.1. Problem Setting

Without loss of generality, Figure 1 shows a typical three-tier supply chain network comprised of two factories, one warehouse and two retail stores. Electric trucks (e-trucks) are employed to move the finished goods from the factories to the warehouse and further down to the stores. Charging stations are placed between two adjacent facilities to recharge the batteries of e-trucks. Microgrid systems consisting of WT, PV, and ESS are installed on site to power the local facilities. All microgrids are inter-connected with the main grid. This enables each facility to realize two-way power flow and participate in energy trading under an aggregation scheme (Bhatia 2014; Koraki and Strunz 2018).

Figure 1: A Three-Tier Supply Chain Network with Microgrid Integration (Place here)

Our goal is to allocate WT, PV and ESS to meet the power demand of local facilities while minimizing the total supply chain cost, including production, inventory, transportation and energy. We propose a mixed-integer programming model for jointly optimizing the production lots and allocating microgrid portfolio and capacity. The model not only makes a strategic production decision to satisfy the uncertain product demand in each period, but also schedules microgrid generation to meet the hourly electricity needs of each facility considering power intermittency. Tables 1 and 2, respectively, list the parameters and the decision variables of the model which will be presented in next section.

Table 1: Model Parameters (Place here)

Table 2: Decision Variables of The Planning Model (Place here)

3.2. Integration of Production Planning and Microgrid Sizing

We formulate an integrated production planning and microgrid sizing (PPMS) model to realize transactive energy operations with minimum cost. There are two primary assumptions of the model. First, the product demands per period are random and independently follow the normal distribution. Second, the trading mechanism of microgrid and utility energy is orchestrated through an aggregation scheme across all the supply chain entities. Figure1 shows a typical three-tier supply chain network comprised of K factories, N warehouses, and S stores. Each factory can produce I products to meet the demand from the retail stores over the planning horizon. $\mathbf{x}$, $\mathbf{y}$, and $\mathbf{z}$ are the decision variables representing the production, inventory, and backorders per period. $\mathbf{P}^c$ represents the WT and PV capacity, $\mathbf{B}^c$ is the ESS size, and $\mathbf{E}$ is the hourly energy transaction. The goal is to make both strategic and operational decisions on production lot, microgrid capacity, and hourly energy trading such that the annual supply chain cost is minimized. The PPMS optimization model is formulated as follows.

Model PPMS

Minimize:

$$
\begin{aligned}
f(\mathbf{x},\mathbf{y},\mathbf{z},\mathbf{P}^c,\mathbf{B}^c,\mathbf{E}) = {} & \sum_{i=1}^{I}\sum_{j=1}^{J}\sum_{k=1}^{K}\sum_{n=1}^{N}(p_{ijk}+\pi_{ikn})x_{ijkn} + \sum_{i=1}^{I}\sum_{j=1}^{J}\sum_{n=1}^{N}h_{ijn}y_{ijn} + \sum_{i=1}^{I}\sum_{j=1}^{J-1}\sum_{n=1}^{N}b_{ijn}z_{ijn} + \sum_{i=1}^{I}\sum_{j=1}^{J}\sum_{n=1}^{N}\sum_{s=1}^{S}\tilde{\pi}_{ins}\tilde{x}_{ijns} \\
& + \sum_{g=1}^{G}\sum_{k=1}^{K}\phi_g a_g P_{gk}^c + \sum_{j=1}^{J}\sum_{t=1}^{T}\sum_{g=1}^{G}\sum_{k=1}^{K}\tau_{gk}(b_g-c_g)\lambda_{jtgk}P_{gk}^c + \varphi_{ES}d_{ES}\sum_{k=1}^{K}B_k^c + \sum_{k=1}^{K}\sum_{j=1}^{J}\sum_{t=1}^{T}(\rho_{kt}^{bu}E_{kt}^{bu} - \rho_{kt}^{se}E_{kt}^{se}) \\
& + \sum_{g=1}^{G}\sum_{n=1}^{N}\phi_g a_g P_{gn}^c + \sum_{j=1}^{J}\sum_{t=1}^{T}\sum_{g=1}^{G}\sum_{n=1}^{N}\tau_{gn}(b_g-c_g)\lambda_{jtgn}P_{gn}^c + \varphi_{ES}d_{ES}\sum_{n=1}^{N}B_n^c + \sum_{n=1}^{N}\sum_{j=1}^{J}\sum_{t=1}^{T}(\rho_{nt}^{bu}E_{nt}^{bu} - \rho_{nt}^{se}E_{nt}^{se}) \\
& + \sum_{g=1}^{G}\sum_{s=1}^{S}\phi_g a_g P_{gs}^c + \sum_{j=1}^{J}\sum_{t=1}^{T}\sum_{g=1}^{G}\sum_{s=1}^{S}\tau_{gs}(b_g-c_g)\lambda_{jtgs}P_{gs}^c + \varphi_{ES}d_{ES}\sum_{s=1}^{S}B_s^c + \sum_{s=1}^{S}\sum_{j=1}^{J}\sum_{t=1}^{T}(\rho_{st}^{bu}E_{st}^{bu} - \rho_{st}^{se}E_{st}^{se})
\end{aligned}
\tag{1}
$$

Subject to:

$$\sum_{k=1}^{K} x_{i1kn} + y_{i0n} - y_{i1n} + z_{i1n} = \sum_{s=1}^{S} \tilde{x}_{i1ns}, \qquad \text{for } j=1, \forall i, \text{ and } \forall n \tag{2}$$

$$\sum_{k=1}^{K} x_{ijkn} + y_{ij-1n} - y_{ijn} - z_{ij-1n} + z_{ijn} = \sum_{s=1}^{S} \tilde{x}_{ijns}, \qquad \text{for } j=2, 3, .., J\text{-}1, \forall i, \text{ and } \forall n \tag{3}$$

$$\sum_{k=1}^{K} x_{iJkn} + y_{iJ-1n} - y_{iJn} - z_{iJ-1n} = \sum_{s=1}^{S} x_{iJns}, \qquad \text{for } j=J, \forall i, \text{ and } \forall n \tag{4}$$

$$\Pr\left\{ \sum_{n=1}^{N} \tilde{x}_{ijns} \geq D_{ijs} \right\} \geq \alpha, \qquad \forall i, \forall j, \text{ and } \forall s \tag{5}$$

$$\sum_{i=1}^{I} \sum_{n=1}^{N} v_{ikr} x_{ijkn} \leq w_{jkr}, \qquad \forall j, \forall k, \text{ and } \forall r \tag{6}$$

$$y_{i0n} = 0, \qquad \forall i \text{ and } \forall n \tag{7}$$

$$\sum_{i=1}^{I} \sum_{n=1}^{N} (e_{ik} + q_v d_{kn} m_i) x^t_{ijkn} + \sum_{n=1}^{N} q_v n_{tkn} d_{kn} w_v + B_{kt} - B_{k,t-1} + E^{se}_{kjt} - E^{bu}_{kjt} = \sum_{g=1}^{G} \tau_{gk} \lambda_{tgk} P^c_{gk},$$

$$\forall t, \forall j, \text{ and } \forall k \tag{8}$$

$$\tau_w L_n + \sum_{k=1}^{K} q_v n_{jtkn} d_{kn} w_v + \sum_{i=1}^{I} \sum_{s=1}^{S} q_v \tilde{d}_{jtns} m_i \tilde{x}^t_{ijns} + \sum_{s=1}^{S} q_v \tilde{n}_{jtns} \tilde{d}_{ns} w_v + B_{njt} - B_{nj,t-1} + E^{se}_{njt} - E^{bu}_{njt} = \sum_{g=1}^{G} \tau_{gn} \lambda_{jtgn} P^c_{gn},$$

$$\forall t, \forall j, \text{ and } \forall n \tag{9}$$

$$\tilde{\tau}_s \tilde{L}_s + \sum_{n=1}^{N} q_v \tilde{n}_{jtns} \tilde{d}_{ns} w_v + B_{sjt} - B_{s,jt-1} + E^{se}_{sjt} - E^{bu}_{sjt} = \sum_{g=1}^{G} \tau_{gs} \lambda_{jtgs} P^c_{gs}, \qquad \forall t, \forall j, \text{ and } \forall s \tag{10}$$

$$x^t_{ijkn} = \frac{x_{ijkn}}{T}, \qquad \forall t, \ \forall i, \forall j, \forall k, \text{ and } \forall n \tag{11}$$

$$\tilde{x}^t_{ijns} = \frac{\tilde{x}_{ijns}}{T}, \qquad \forall t, \ \forall i, \forall j, \forall k, \text{ and } \forall n \tag{12}$$

$$0 \leq B_{kjt} \leq B^c_k, \qquad \forall \text{t}, \forall \text{j}, \text{ and } \forall \text{k} \tag{13}$$

$$0 \le B_{njt} \le B_n^c, \qquad \forall t, \forall j, \text{ and } \forall k \tag{14}$$

$$0 \le B_{sjt} \le B_s^c, \qquad \forall t, \forall j, \text{ and } \forall k \tag{15}$$

$$B_{kj0} = B_{kj-1T}, \qquad \text{for } j = 2,3,\ldots,J, \text{ and } \forall k \tag{16}$$

$$B_{nj0} = B_{nj-1T}, \qquad \text{for } j = 2,3,\ldots,J, \text{ and } \forall k \tag{17}$$

$$B_{sj0} = B_{sj-1T}, \qquad \text{for } j = 2,3,\ldots,J, \text{ and } \forall k \tag{18}$$

$$B_{k,1,0}, B_{kJT} = B_k^c, \qquad \forall k \tag{19}$$

$$B_{n,1,0}, B_{nJT} = B_n^c, \qquad \forall n \tag{20}$$

$$B_{s,1,0}, B_{sJT} = B_s^c, \qquad \forall s \tag{21}$$

$$0 \le P_{gk}^c, P_{gn}^c, P_{gs}^c \le P_{\max}^c, \qquad \forall g, \forall k, \forall n, \text{ and } \forall s \tag{22}$$

$$E_{kjt}^{bu}, E_{kjt}^{se} \ge 0, \qquad \forall t, \forall j, \text{ and } \forall k \tag{23}$$

$$E_{njt}^{bu}, E_{njt}^{se} \ge 0, \qquad \forall t, \forall j, \text{ and } \forall n \tag{24}$$

$$E_{sjt}^{bu}, E_{sjt}^{se} \ge 0, \qquad \forall t, \forall j, \text{ and } \forall s \tag{25}$$

$$B_k^c, B_n^c, B_s^c \ge 0, \qquad \forall k, \forall n, \text{ and } \forall s \tag{26}$$

$$B_{kjt}, B_{njt}, B_{sjt} \ge 0, \qquad \forall t, \forall j, \forall k, \forall n, \text{ and } \forall s \tag{27}$$

$$x_{ijkn}, \tilde{x}_{ijns}, y_{ijn}, z_{ijn} \ge 0, \qquad \forall t, \forall i, \forall j, \forall k, \forall n, \text{ and } \forall s \tag{28}$$

Objective function (1) aims to minimize the operation cost comprised of production, transportation, inventory, backorders, and energy over J periods. Note that λ_{jtgk} represents the capacity factor of renewable generation g. It is a random variable depending on the wind speed or

sunshine condition at time t of period j in factory k. Hence the actual output power is $\lambda_{jtgk}P^c_{gk}$ where P^c_{gk} is the capacity of generation g in factory k. Same interpretation can be applied to warehouses and stores.

Constraints (2) to (4) are the production-inventory balance equations between factories and warehouses for each product in each period. Constraint (5) is the chance constraint and states that for given product i in period j, the demand of store s must be satisfied at $100\times\alpha\%$ confidence level. Constraint (6) represents the production resource constraint, such as labor and machine hours available in each period. Constraint (7) assumes the initial inventory is zero. Constraint (8) is the hourly energy balance equation in factory. For factory k, the hourly electricity load, the forward electric transportation, the stored energy, and the transactive energy between microgrid and main grid are offset by onsite generation. Similarly, constraints (9) and (10) define the hourly energy balance at warehouses and retail stores, respectively. Constraints (11) and (12) convert the strategic production decision into hourly production rate, and T is the number of hours per production period. Constraints (13) to (15) state that the energy stored in the ESS should not exceed its capacity limit. Constraints (16) to (18) indicate that the initial ESS state at the beginning of the current period must be equal to the state of the last hour of the previous period. Constraint (19) to (21) state that the ESS is full at the beginning and the end of the planning horizon. Constraint (22) defines the lower and upper limits of output power of generation g. Constraints (23) to (28) indicate the non-negativity requirement of the decision variables.

Model PPMS belongs to the stochastic optimization problem because of the chance constraint (5) and random capacity factors λ_{jtgk}, λ_{jtgn}, and λ_{jtgs}. Normality assumption on product demands is often used in literature (Mula et al. 2006; Kok et al. 2018). If the product demand is

normally distributed, the chance constraint can be converted into its deterministic counterpart as follows

$$\sum_{n=1}^{N} \tilde{x}_{ijns} \geq \mu_{ijs} + z_{\alpha}\sigma_{ijs}, \quad \forall i, \forall j, \text{and } \forall s \tag{29}$$

where, μ_{ijs} and σ_{ijs} are the mean and standard deviation of D_{ijs}. Note that z_{α} is the z-value of the standard normal distribution with probability α. Below we further characterize the random capacity factors based on 11-year hourly meteorological data. Our intention is to convert Model PPMS into a mixed-integer linear optimization problem that can be solved by commercially available solvers.

4. Hourly WT and PV Capacity Factor

Capacity factor (CF) is defined as the ratio between the actual output power of a WT or PV system versus its capacity limit. CF value varies between 0 and 1 depending on the wind speed or sunshine conditions at time t of period j. Table 3 lists the name and location of ten cities for the implementation of Model PPMS. These cities are chosen because they represent a wide range of climate conditions. The hourly wind speed and weather states of each city from 2006 to 2016 are retrieved from the web portal of Weather Underground with total of 192,192 records (Weather Underground 2017). The aggregate climate data size of ten cities reaches 1.92 million. This allows for the accurate estimation of the hourly CF values. The average CF of WT and PV for each city is summarized in Table 3.

Table 3: Average Capacity Factor of WT and PV of Ten US Cities (Place here)

Based on the mean CF values in Table 3, wind and solar generation is classified into three categories: low if CF<0.2, medium if 0.2≤CF<0.4, and high if CF≥0.4. For instance, Tucson has

the strongest solar generation with CF=0.46 whereas the solar CF in Salt Lake City is only 0.22. If a 2 MW PV is installed in Tucson, the average power output is 0.46×2=0.92 MW. The same PV system in Salt Lake City only generates 0.22×2=0.44 MW. Similar interpretation can be applied to WT based on the CF value in the table.

The hourly CF values of WT and PV of ten cities from January to December are plotted in Figure 2. Since the CF values are estimated based on 11-year hourly meteorological data, they represent the average value of a particular hour. A common observation is that PV capacity factor exhibits a seasonal pattern. It is low in the winter and reaches the highest in the summer season. It is worth mentioning that CF=0 for PV in the night hours. The seasonality of WT capacity factor is also observed in Phoenix, Salt Lake City, and San Francisco. For instance, the wind CF in San Francisco is low with less than 0.17 in January and February. It increases and reaches the peak level of 0.83 in May, and then remains at a stable level from June to August before declining to 0.2 in December.

Figure 2: Hourly Capacity Factor of WT and PV from January to December (Place here)

5. Numerical Experiment on Five-Facility Supply Chain

5.1. Two-Factory, One-Warehouse, and Two-Store Network

First, we design a three-tier manufacturing supply chain comprised two factories, one warehouse and two stores, or denoted as 2F-1W-2S. The network layout including the mileage between adjacent cities is available in Figure 1. Factories 1 and 2 are located in Phoenix and Reno, respectively. Las Vegas is the site for the warehouse. Stores 1 and 2 are located in Salt Lake City and San Jose, respectively.

Table 4: Weekly Product Demands from Stores 1 and 2 (Place here)

Each factory makes two products, A and B. The production planning is scheduled on a weekly basis over 52 weeks or one year. The mean and standard deviation of weekly demands in Stores 1 and 2 are available in Table 4. In addition, the demand in each store must be met with α=90% confidence. Parameters such as energy use, resource consumption, inventory overhead, and transportation cost are given in Table 5. These values are appropriately estimated from energy-intensive industries that draw electric power in 24/7 mode, such as semiconductor manufacturing, air separation process or oil refinery plant. The available machine and labor hours per week in each factory are shown in Table A1 of Appendix.

Table 5: Parameters for Production Planning for 2F-1F-2S (Place here)

Table 6: Parameters for Microgrid Sizing for 2F-1F-2S (Place here)

Table 6 further provides the model input data for WT, PV, ESS, e-trucks and utility power. Though variations may exist, these values are adopted or estimated based on the reports from National Renewable Energy Laboratory (Stehly et al. 2018; Fu et al. 2018a; Fu et al. 2018b). The capital recovery factor of WT and PV, ϕ_g, is estimated assuming 20 years lifetime with 5% discount rate. For ESS, φ_{ES} is estimated assuming 10 years lifetime with 5% discount rate. Factories operate in 24 hours a day and 7 days a week (i.e., 24/7 mode), and the electric load of a factory depends on the production rate of Products A and B. The warehouse in Las Vegas operates in 24/7 mode with relatively stable load of 7 MW. The two stores open in the daytime only with 12 hours/day, and the average power load of each store is assumed to be 4 MW.

5.2. Results of Production Planning

Model PPMS is solved to determine the weekly production over one-year period for the 2F-1W-2S network. The model contains 132,359 decision variables and 88,563 constraints, and is coded with Advanced Mathematical Programming Language (AMPL). Cplex solver is used to search for

the optimal solution for minimizing $f(\mathbf{x}, \mathbf{y}, \mathbf{z}, \mathbf{P}^c, \mathbf{B}^c, \mathbf{E})$. The AMPL code is executed in Intel(R) Core(TM) i5-7200U CPU @ 2.5GHz, 4 Core(s), 24 GB memory, 4 Logical Processors with running time of 21 seconds. Excluding the energy cost, the 52-week production cost is found with $f_p(\mathbf{x}, \mathbf{y}, \mathbf{z})$=\$70,056,330 where $f_p(\mathbf{x}, \mathbf{y}, \mathbf{z})$ corresponds to the first row of objective function (1). Figure 3 depicts the weekly decisions on **x**, **y** and **z** of Products A and B, respectively. Since the backorder cost is relatively high for both products, the model returns a solution with small amounts of backorders.

Figure 3: Production and Inventory Decisions of the 2F-1W-2S Network

Sensitivity analysis is performed to investigate how the holding and the backorder costs influence the production lots. The cost of Products A and B varies by 50% with respect to the benchmark values in Table 5. Model PPMS is solved again, and Table 7 shows the new results in comparison to the benchmark cost. It is found that the relative cost difference is quite small and between -0.57% and 0.51%. Hence the production decision based on Model PPMS is robust regardless of relatively large variations in holding or backorder cost.

Table 7: Sensitivity Analysis on Production Planning for 2F-1F-2S (Place here)

5.3. Results of Microgrid Sizing

Table 8 summarizes the optimal sizing of WT, PV and ESS for each facility of the 2F-1W-2S network. The total supply chain cost $f(\mathbf{x}, \mathbf{y}, \mathbf{z}, \mathbf{P}^c, \mathbf{B}^c, \mathbf{E})$ is \$87,207,113. The energy cost is $f(\mathbf{x}, \mathbf{y}, \mathbf{z}, \mathbf{P}^c, \mathbf{B}^c, \mathbf{E}) - f_p(\mathbf{x}, \mathbf{y}, \mathbf{z})$ =\$17,150,783, representing 20% of the total annual cost.

Table 8: Sizing of WT, PV and ESS for 2F-1W-2S (Place here)

The warehouse in Las Vegas opts to install 3.18 MW WT and 7.08 MW PV. The store in Salt Lake City installs 4.27 MW WT. There are no microgrid installation in Phoenix, Reno, and San Jose. Rather, these locations prefer to power the facilities using the main grid. If we examine

the capacity factor in Table 3, Las Vegas and Salt Lake City possess medium wind CF whereas it is below 0.17 in other three cities. The CF of PV in Las Vegas is the largest with 0.43 among the five cities. Given the electricity buying price of $70/MWh, it is more economical for Phoenix, Reno and San Jose to use grid power.

Figure 4 shows the hourly energy purchased from and sold to the grid for the warehouse in Las Vegas over the year and in Week 29, respectively. The warehouse is able to engage transactive energy trading because of onsite WT and PV generation. Figure 5 shows the power flow of the factories and stores in other four locations. The factories in Phoenix and Reno use the grid power because of no microgrid installation. The fluctuation of the power demand is caused by the production lot variation in each week. The store in Salt Lake City chooses to install WT due to high wind CF, and any power deficit is met by the main grid. Meanwhile, in days with higher WT throughput, the excess energy is sold to the main grid in the TE market. For the store in San Jose, the required energy is fulfilled by the main grid because of no microgrid installation.

Figure 4: Prosumer Energy Trading in Las Vegas Warehouse (Place here)

Figure 5: Hourly Energy Transactions in Factories and Stores (Place here)

5.4. Sensitivity Analysis of Microgrid Sizing

Sensitivity analysis is performed by varying the microgrid parameters, including energy selling and buying price, time-of-use (TOU) rate, battery capacity cost, transactive energy amount, and PV installation cost. Eight variants are generated and compared with the benchmark (i.e., Case 1). The costs of each variant are summarized in Table 9, and the microgrid sizing is depicted in Figure 6. Three observations can be made from Table 9. First, by comparing Cases 2 with 3, the electricty buying price has a major impact on the supply chain cost. In Case 3, when the buying price of all facilities increases from 70 to $140/MWh, the total cost increases by 12.3%. In Case 4 when the

TOU rate is $140/MWh from 10am to 9pm, the total cost goes up by 5.4%. Second, Cases 5 shows that reducing the ESS cost from $0.4M/MWh to $0.01/MWh has limited impact on the adoption of this technology. In Case 6, a maximum amount of transactive power is imposed on each facility. For instance, the maxium power a factory can purchase from the grid is 8 MW or equvillently 8 MWh per hour. Similarly the maximum power exorpoted to the grid is capped by 8 MW. Figure 6e shows ESS becomes preferable for installation, yet the total supply chain cost only incases by 0.6%. Both Cases 5 and 6 show that the adoption of ESS is closely related with the maximum limit of the transactive energy being trading. Results of Cases 7-9 are further elaborated next.

Table 9: Cost Comparisons between Different Cases for 2F-1F-2S (Place here)

Next we compare the microgrid portfolio and sizing between the benchmark and the eight variants. From Figure 6, five observations are made and summarized below.

- Energy selling price has limited impact on the aggregate microgrid capacity. In Case 2 of Figure 6a, when the energy selling price is reduced by 50%, the WT size in Las Vegas reduces but its PV capacity increases. The WT sizing in Salt Lake City remains almost the same as in Case 1.
- Energy buying price has a major impact on the microgrid portfolio and sizing. In Case 3 of Figure 6b when the buying cost doubles, Phoenix, Reno and San Jose opt to install onsite generation. Meanwhile, the microgrid capacity in Las Vegas and Salt Lake City also increase compared to Case 1. A similar observation can be made under TOU of Case 4 in Figure 6c where ESS units are installed in Phoenix, Reno and San Jose. This means TOU not only motivates the renewables installation, but also stimulates the use of ESS.
- Under the flat rate of $70/MWh, Case 5 in Figure 6d shows that ESS becomes attractive in Las Vegas when its cost drops to $0.01M/MWh as opposed to the current $0.4M/MWh. In

Case 6 when a maximum transactive power limit is imposed, all locations except Salt Lake city start to install ESS units as shown Figure 6e.

- For Case 7 in Figure 6f, if the PV capacity cost decreases from $2M/MW to $1M/MW, all these locations choose to install PV even if the energy selling price is $0/MWh.
- In Cases 8, if the utility price in Reno increases to $140/MWh while other cities remain at $70/MWh, both WT and PV are adopted in Reno. In Case 9, if the TOU rate is adopted in Reno, only PV is installed to handle the higher electricity price in the daytime. In the night the factory can be powered with low-price grid energy. For both Cases 8 and 9, there is no change in microgrid sizing of other locations as shown in Figure 6g and 6h, respectively.

Figure 6: Microgrid Sizing for Cases 2 to 7 (Place here)

6. Numerical Experiment on Ten-Facility Supply Chain

6.1. Four-Factory, Two-Warehouse, and Four-Store Network

To examine the scalability, Model PPMS is implemented in a larger supply chain network with 10-facility shown in Figure 7. The 4F-2W-4S network is comprised of four factories, two warehouses and, and four stores. The four factories are located in Phoenix, Reno, Yuma and Tucson, respectively. The two warehouses are located in Las Vegas and Los Angles, and the four stores are in Salt Lake City, San Jose, Sacramento and San Francisco, respectively. A microgrid, if installed, is connected with the main grid.

Figure 7: A 4-Factory, 2-Warehouse and 4-Store Supply Chain (Place here)

Table 10: Weekly Product Demand of the 4F-2W-4S Network (Place here)

Table 10 shows the mean and standard deviation of the weekly demand of Products A and B in four stores. The availability of weekly labor and machine hours in each factory is shown in

Table A2 of Appendix. For this 4F-2W-4S network, there are 266,382 decision variables and 177,958 constraints. Solving the model results in the production cost $f_p(\mathbf{x}, \mathbf{y}, \mathbf{z})$ =$82,508,887. Figures 8 shows the weekly production lots in four factories, as well as the inventory and backorders in two warehouses.

Figure 8: Production and Inventory Planning for the 4F-2W-4S Network (Place here)

6.2. Microgrid Sizing

The WT, PV and ESS sizing for each facility is presented in Table 11. Factory 4 in Tucson installs 6.41MW PV. Warehouse 1 in Las Vegas installs 3.18 MW WT and 7.09 MW PV, and Warehouse 2 in Los Angeles installs 7.02 MW WT. Store 1 in Salt Lake City and Store 4 in San Francisco install 4.28 MW and 18 MW WT, respectively. Other facilities with no microgrid are powered by the main grid. The objective function $f(\mathbf{x}, \mathbf{y}, \mathbf{z}, \mathbf{P}^c, \mathbf{B}^c, \mathbf{E})$= $108,085,946, among which $25,577,000 is the energy cost, representing 23.7% of the total supply chain cost.

Table 11: Microgrid Sizing of 4F-2W-4S Network for the Benchmark Study (Case 1) (Place here)

7. Conclusion

This paper proposes an integrated planning model to allocate production quantity and microgrid capacity for transactive energy trading in a three-tier supply chain infrastructure. Under product demand and power supply uncertainty, the model performs strategic decisions on production, inventory and renewable capacity, as well as operational decisions on power scheduling and transaction for minimizing the total supply chain cost. The study contributes to the design and application of sustainable supply chain infrastructure in that it incorporates distributed energy resources into classical production-inventory model for achieving three outcomes: environmental sustainability, energy independence, and prosumer economy. The proposed model represents an

early attempt to encompass four supply chain features, i.e., materials, information, cash and transactive energy flows, under a unified decision-making framework. The model is demonstrated on two network instances comprised of up to ten facilities across a large US region with diverse climate conditions. Several managerial insights are derived. First, time-of-use rate has a significant impact on the allocation of renewable portfolio and microgrid capacity. When the daytime electricity price is twice of the off-peak rate, it motivates the installation of wind turbine, solar photovoltaics, and energy storage units. Second, given current battery cost of $0.3-0.4M/MWh, it is not cost-effective for large scale use in grid-tied microgrid mode. However, battery system becomes competitive if a maximum amount of transactive energy is imposed on microgrid. Third, if PV capacity cost decreases from $2M/MW to $1M/MW, it could compete with the utility price of $70/MWh even under zero feed-in tariff rate. For future study the current model could be extended in several directions. For instance, it is interesting to exmine how the microgrid sizing and output affect the material flow and backorders in the supply chain. Another direction is how the renewable energy characteristics of different locations affect the electric vehicle routing. In addition, prosumers can also leverage blockchain technology to create secured and smart contracts, and directly engage peer-to-peer trading without a centralized energy market.

Appendix

A1. Available Labor and Machine Hours for 2F-1W-2S Network

Table A1: Resource Data for 2F-1W-2S Network (Note: F1=Factory 1, F2=Factory 2) (Place here)

A2. Available Labor and Machine Hours for 4F-2W-4S Network

Table A2: Resource Data for 4F-2W-4S Network for Weeks 1-26 (Place here)

Table A2: Resource Data for 4F-2W-4S Network for Weeks 27-52 (Continued) (Place here)

Acknowledgement

This research is supported by the U.S. National Science Foundation under the Chemical, Bioengineering, Environmental, and Transport Systems (CBET) program (award # 1704933)

References:

- Abdallah, T, Diabat, A, Rigter, J (2013). Investigating the option of installing small scale PVs on facility rooftops in a green supply chain. International Journal of Production Economics, vol. 146, no. 2, pp. 465-477.
- Bhatia, SC (2014). Cogeneration. Chapter 19, Advanced Renewable Energy Systems, 2014. Available at https://www.sciencedirect.com/topics/engineering/heat-to-power-ratio (accessed on July 5, 2019).
- Cheng, F, Ettl, M, Lu, Y, Yao, DD (2012). A production-inventory model for a push-pull manufacturing system with capacity and service level constraints. Production and Operations Management, vol. 21, no. 4, pp. 668-681.
- DOE, (2015), GridWise Transactive Energy Framework, Version 1.0, Report by The U.S. Department of Energy's Gridwise Architecture Council, January 2015, available at https://www.gridwiseac.org/pdfs/te_framework_report_pnnl-22946.pdf, (accessed on January 13, 2022).
- Drake, DF, Kleindorfer, PR, Van Wassenhove, LN (2016). Technology choice and capacity portfolios under emissions regulation. Production and Operations Management, vol. 25, no. 6, pp. 1006-1025.
- EIA (2019). Annual Energy Outlook 2019 with Projections to 2050. Reported by U.S. Energy Information Administration (EIA), U.S. Department of Energy, Washington, DC 20585, https://www.eia.gov/aeo, (accessed on March 19, 2020).
- Fu, R, Feldman, D, Margolis, R, Woodhouse, M, Ardani, K (2018). The U.S. Solar Photovoltaic System Cost Benchmark: Q1 2017. National Renewable Energy Laboratory Report. Available at https://www.nrel.gov/docs/fy17osti/68925.pdf, (accessed on September 4, 2019).
- Fu, R, Remo, T, Margolis, R (2018). The 2018 U.S. Utility-scale Photovoltaics-Plus-Energy Storage System Costs Benchmark. National Renewable Energy Laboratory Report. Available at https://www.nrel.gov/docs/fy19osti/71714.pdf, (accessed on September 4, 2019).

- Golari, M, Fan, N, Jin, T (2017). Multistage stochastic optimization for production-inventory planning with intermittent renewable energy. Production and Operations Management, vol. 26, no. 3, pp. 409-425.
- Gong, X, Zhou, SX (2013). Optimal production planning with emissions trading. Operations Research, vol. 61, no. 4, pp. 908-924.
- Goodarzi, S., Aflaki, S., Masini, A. (2019) Optimal feed-in tariff policies: The impact of market structure and technology characteristics. Production and Operations Management, vol. 28, no. 5, pp. 1108-1128.
- Guerrero, J, Gebbran, D, Mhanna, S, Chapman, AC, Verbič, G (2020). Towards a transactive energy system for integration of distributed energy resources: Home energy management, distributed optimal power flow, and peer-to-peer energy trading. Renewable and Sustainable Energy Reviews, vol. 132, p. 110000. https://doi.org/10.1016/j.rser.2020.110000.
- He, P, Dou, G, Zhang, W, (2017). Optimal production planning and cap setting under cap-and-trade regulation. Journal of the Operational Research Society, vol. 68, no. 9, pp. 1094-1105.
- Huddleston Jr., T (2015). Google's latest renewable energy investment is its biggest ever. Fortune, reported on December 3, 2015. Available at http://fortune.com/2015/12/03/google-renewable-energy/, (accessed on January 10, 2020).
- Karen, K, George, YG, Liu, YH (2004). Stochastic modeling for inventory and production planning in the paper industry. American Institute of Chemical Engineers Journal, vol. 50, no. 11, pp. 2877-2890.
- Kok, T, Grob, C, Laumanns, M, Minner, S, Rambau, J, Schade, K (2018). A typology and literature review on stochastic multi-echelon inventory models. European Journal of Operational Research, vol. 269, no. 3, pp. 955-983.
- Koraki, D, Strunz, K, (2018). Wind and solar power integration in electricity markets and distribution networks through service-centric virtual power plants. IEEE Transactions on Power Systems, vol. 33, no. 1, pp. 473-485.
- Lee, J-Y, (2020). Investing in carbon emissions reduction in the EOQ model. Journal of the Operational Research Society, vol. 71, no. 8, pp. 1289-1300.
- Li, B, Tian, Y, Chen, F, Jin, T (2017). Toward net-zero carbon manufacturing operations: an onsite renewables solution. Journal of the Operational Research Society, vol. 68, no. 3, pp. 308-321.

- Malhotra, A, Battke, B, Beuse, M, Stephan, A, Schmidt, T (2016). Use cases for stationary battery technologies: A review of the literature and existing projects. Renewable and Sustainable Energy Reviews, vol. 56, pp. 705-721.
- Martin, R (2012). Revenue from virtual power plants will reach $5.3 billion by 2017. Business Wire, Forecasts Pike Research (Press release). Reported on 18 April 2012. Available https://www.businesswire.com/news/, (accessed April 4, 2019)
- Megahed, A, Goetschalckx, M (2018). Tactical supply chain planning under uncertainty with an application in the wind turbines industry. Computers & Operations Research, vol. 100, December issue, pp. 287-300.
- Mula, J, Poler, R, Garca-Sabater, JP, Lario, FC (2006). Models for production planning under uncertainty: A review. International Journal of Production Economics, vol. 103, no. 1, pp. 271-285.
- Ozment, D (2014). Walmart's Commitment to Solar. Reported on May 9, 2014. Available at http://blog.walmart.com/sustainability/20140509/walmarts-commitment-to-solar, (accessed on December 19, 2019).
- Pan, X, Li, M, Xu, H, Guo, S, Guo, R, Lee, C T (2021). Simulation on the effectiveness of carbon emission trading policy: A system dynamics approach. Journal of the Operational Research Society, vol. 72, no. 7, pp. 1447-1460.
- Parker, GG, Tan, B, Kazan, O (2019). Electric power industry: Operational and public policy challenges and opportunities. Production and Operations Management, vol. 28, no. 11, pp. 2738-2777.
- Pham, A, Jin, T, Novoa, C, Qin, J (2019). A multi-site production and microgrid planning model for net-zero energy operations. International Journal of Production Economics, vol. 218, December issue, pp. 260-274.
- Progressive Grocer (2019). Walmart to add solar energy at 46 Stores. Reported on May, 9, 2019. Available at https://progressivegrocer.com/walmart-add-solar-energy-46-stores, (accessed on April 2, 2020).
- Sæther, G, Crespo del Granado, P, Zaferanlouei, S (2021). Peer-to-peer electricity trading in an industrial site: Value of buildings flexibility on peak load reduction. Energy and Buildings, vol. 236, p. 110737. https://doi.org/10.1016/j.enbuild.2021.110737.
- Sox, CR, Muckstadt, JA (1996). Multi-item, multi-period production planning with uncertain demand. IIE Transactions, vol. 28, no. 11, pp. 891-900.

- Stehly, T, Beiter, P, Heimiller, D, Scott, G (2018). The 2017 Cost of Wind Energy Review. National Renewable Energy Laboratory Report. Available at https://www.nrel.gov/docs/fy18osti/72167.pdf, (accessed on September 10, 2019).
- Stinpetru, L (2014). Honda Installs Wind Turbines at Manufacturing Plant in Ohio, US. Reported on January 23, 2014. Available at http://news.softpedia.com/news/Honda-Installs-Wind-Turbines-at-Manufacturing-Plant-in-Ohio-US-419798.shtml, (accessed on March 3, 2015).
- Tan, B, Gershwin, SB (2004). Production and subcontracting strategies for manufacturers with limited capacity and volatile demand. Annals of Operations Research, vol. 125, pp. 205-232.
- Tsao, Y-C, Vu, T-L (2021). A decentralized microgrid considering blockchain adoption and credit risk. Journal of the Operational Research Society, online on August 11, 2021, available at https://doi.org/10.1080/01605682.2021.1960907.
- Yano, CA, Lee, HL (1995). Lot sizing with random yields: A review. Operations Research, vol. 43, no. 2, pp. 311-334.
- Zhang, W, Hua, Z, Xia, Y, Huo, B (2016). Dynamic multi-technology production-inventory problem with emissions trading. IIE Transactions, vol. 48, no. 2, pp. 110-119.
- Zhang, M, Küçükyavuz, S, Yaman, H (2012). A polyhedral study of multiechelon lot sizing with intermediate demands. Operations Research, vol. 60, no. 4, pp. 918-935.

Manuscript Title:

Supply Chain Design for Transactive Energy Operations in the Nexus of Manufacturing, Microgrid and Climate

Table 1: Model Parameters

Notation	Comments
I	number of product type, for i=1, 2, .., I.
J	number of production period, for j=1, 2, .., J.
K	number of factory, for k=1, 2, .., K.
N	number of warehouse, for n=1, 2, .., N.
S	number of retail stores, for s=1, 2, .., S.
R	number of required production resources, for r=1, 2, .., R.
T	the number of power scheduling periods, for t=1, 2, …, T.
G	type of renewable generation, for g=1, 2, .., G.
p_{ijk}	cost of making one unit of product i in period j at factory k ($/item).
h_{ijn}	holding cost of product i in period j at warehouse n ($/item/period).
b_{ijn}	backorder cost of product i in period j at warehouse n ($/item).
π_{ikn}	shipping cost of product i from factory k to warehouse n ($/item/km).
$\tilde{\pi}_{ins}$	shipping cost of product i from warehouse n to store s ($/item/km).
v_{ikr}	resource r consumed for making one unit of product i at factory k.
w_{jkr}	available production resource r in period j at factory k.
D_{ijs}	random demand for product i in period j from store s.
μ_{ijs}, σ_{ijs}	mean and standard deviation of D_{ijs}.
α	probability of meeting the customer product demand (e.g., 0.9 or 0.95).
τ	time step size of power generation scheduling.
τ_{gk}	operating time of generation g at factory k in a production period.
τ_{gn}	operating time of generation g at warehouse n in a production period.
τ_{gs}	operating time of generation g at store s in a production period.
τ_p	time step size of a production period.
a_g	capacity cost of renewable generation g ($/MW).
d_{ES}	capacity cost of energy storage system ($/MWh).
b_{gk}	operation and maintenance cost of generation g at factory k ($/MWh).
b_{gn}	operation and maintenance cost of generation g at warehouse n ($/MWh).
b_{gs}	operation and maintenance cost of generation g at store s ($/MWh).
c_{gk}	carbon credits of generation g at factory k ($/MWh).
c_{gn}	carbon credits of generation g at warehouse n ($/MWh).
c_{gs}	carbon credits of generation g at store s ($/MWh).

ϕ_g capital recovery factor of generation *g*.
φ_{ES} capital recovery factor of energy storage system.
λ_{gkjt} capacity factor of generation *g* for factory *k* in period *j* at time *t*.
λ_{gnjt} capacity factor of generation *g* for warehouse *n* in period *j* at time *t*.
λ_{gsjt} capacity factor of generation *g* for store *s* in period *j* at time *t*.
ρ^{bu}_{kjt} price of buying electricity by factory *k* in period *j* at time *t* ($/MWh).
ρ^{se}_{kjt} price of selling electricity from factory *k* in period *j* at time *t* ($/MWh).
ρ^{bu}_{njt} price of buying electricity by warehouse *n* in period *j* at time *t* ($/MWh).
ρ^{se}_{njt} price of selling electricity from warehouse *n* in period *j* at time *t* ($/MWh).
ρ^{bu}_{sjt} price of buying electricity by store *s* in period *j* at time *t* ($/MWh).
ρ^{se}_{sjt} price of selling electricity from store *s* in period *j* at time *t* ($/MWh).
m_i unit weight of product type *i* (kg/item).
e_{ik} energy use for making one unit of product *i* at facility *k* (MWh/unit).
q_v e-truck electricity intensity rate (MWh/kg/km).
w_v e-truck self-weight (kg).
d_{kn} distance between factory *k* and warehouse *n* (km).
$\tilde{d}_{ns}$ distance between warehouse *n* and store *s* (km).
n_{jtkn} number of trips between factory *k* and warehouse *n* in period *j* at time *t*.
$\tilde{n}_{jstns}$ number of trips between warehouse *n* and store *k* in period *j* at time *t*.
τ_w operating hours of warehouse *n* at time *t*.
$\tilde{\tau}_s$ operating hours of store *s* at time *t*.
L_n power load of warehouse *n* (MW).
$\tilde{L}_s$ power load of store *s* (MW).
$P^c_{\max}$ maximum power capacity (MW).

Table 2: Decision Variables of The Planning Model

Notation	Comments
x_{ijkn}	number of product i in period j made by factory k shipped to warehouse n.
$\tilde{x}_{ijns}$	number of product i in period j shipped from warehouse n to store s.
y_{ijn}	inventory of product i in period j at warehouse n.
z_{ijn}	backorder of product i in period j at warehouse n.
x^t_{ijkn}	amount of product i made by factory k shipped to warehouse n in period j at time t.
$\tilde{x}^t_{ijns}$	amount of product i from warehouse n shipped to store s in period j at time t.
P^c_{gk}	power capacity of generation g at factory k (MW).
P^c_{gn}	power capacity of generation g at warehouse n (MW).
P^c_{gs}	power capacity of generation g at store s (MW).
B^c_k	capacity of ESS at factory k (MWh).
B^c_n	capacity of ESS at warehouse n (MWh).
B^c_s	capacity of ESS at store s (MWh).
B_{kjt}	energy stored in ESS at factory k in period j at time t (MWh).
B_{njt}	energy stored in ESS at warehouse n in period j at time t (MWh).
B_{sjt}	energy stored in ESS at store s in period j at time t (MWh).
E^{bu}_{kjt}	energy bought by factory k in period j at time t (MWh).
E^{se}_{kjt}	energy sold from factory k in period j at time t (MWh).
E^{bu}_{njt}	energy bought by warehouse k in period j at time t (MWh).
E^{se}_{njt}	energy sold from warehouse n in period j at time t (MWh).
E^{bu}_{sjt}	energy bought by store s in period j at time t (MWh).
E^{se}_{sjt}	energy sold from store s in period j at time t (MWh).

Table 3: Average Capacity Factor of WT and PV of Ten US Cities

		Wind Turbine		Solar PV	
No	City and State	Average CF	Category	Average CF	Category
1	Phoenix, AZ	0.12	Low	0.32	Medium
2	Reno, NV	0.17	Low	0.35	Medium
3	Yuma, AZ	0.22	Medium	0.38	Medium
4	Tucson, AZ	0.17	Low	0.46	High
5	Las Vegas, NV	0.24	Medium	0.43	High
6	Los Angeles, CA	0.16	Low	0.28	Medium
7	Salt Lake City, UT	0.26	Medium	0.22	Medium
8	San Jose, CA	0.14	Low	0.31	Medium
9	Sacramento, CA	0.23	Medium	0.42	High
10	San Francisco, CA	0.46	High	0.24	Medium

Table 4: Weekly Product Demands from Stores 1 and 2

	Product A		Product B	
	Mean	Standard Deviation	Mean	Standard Deviation
Store 1	600	55	500	70
Store 2	350	60	400	50

Table 5: Parameters for Production Planning in Model 1

Comments	Notation	Product A (i=1)	Product B (i=2)	Unit
Energy use	e_i	0.9	1.2	MWh/item
Production cost	p_i	400	600	$/item
Holding cost	h_i	16	24	$/item/week
Backorder cost	b_i	75	100	$/item
Shipping cost	π_i	0.05	0.08	$/item/km
Labor hour	v_{i1}	16	24	hour/item
Machine hour	v_{i2}	100	200	hour/item
Product weight	m_i	3	4	kg/item

Table 6: Parameters for Microgrid Sizing in Model 2

DG	Notation	Value	Unit	Notation	Value	Unit
WT	a_g	1.5	\$M/MW	w_v	5000	kg
WT	b_g	12	\$/MWh	q_v	1.19×10^{-7}	MWh/kg/km
WT	c_g	0	\$/MWh	T	168	hour/period
WT	ϕ_g	0.0802	n/a	n_{tkn}, $\tilde{n}_{tns}$	1	trip/week
PV	a_g	1.9	\$M/MW	τ_w	1	hour
PV	b_g	4	\$/MWh	$\tilde{\tau}_s$	1	hour
PV	c_g	10	\$MWh	P^c_{max}	18	MW
PV	ϕ_g	0.0802	n/a	τ_{gk}, τ_{gn}, τ_{gs}	1	hour
ESS	d_{ES}	0.4	\$M/MWh	ρ^{bu}_{kt}, ρ^{bu}_{nt}, ρ^{bu}_{st}	70	\$/MWh
ESS	φ_{ES}	0.1295	n/a	ρ^{se}_{kt}, ρ^{se}_{nt}, ρ^{se}_{st}	50	\$/MWh

Table 7: Sensitivity Analysis on Production Planning for the Model

Scenario	$f_p(\mathbf{x}, \mathbf{y}, \mathbf{z})$	Difference ($)	Relative Difference (%)
Benchmark	70,056,330	0	0.00
Increase h_i by 50%	69,656,520	-399,810	-0.57
Decrease h_i by 50%	70,418,506	362,176	0.51
Increase b_i by 50%	69,857,066	-199,264	-0.29
Decrease b_i by 50%	70,199,490	143,160	0.20

Table 8: Sizing of WT, PV and ESS for 2F-1W-2S

DG Type	Phoenix (Factory 1)	Reno (Factory 2)	Las Vegas (Warehouse)	Salt Lake City (Store 1)	San Jose (Store 2)
WT (MW)	0	0	3.18	4.27	0
PV (MW)	0	0	7.08	0	0
ESS (MWh)	0	0	0	0	0

Table 9: Cost Comparisons between Different Cases for 2F-1F-2S

Case	Total supply chain cost	Cost Difference ($)	Difference (%)	Comments
1	87,207,113	0	0	Benchmark
2	87,209,895	2,782	≈0	$25/MWh for selling price
3	97,916,429	10,709,316	12.3	$140/MWh for buying price
4	91,911,500	4,704,387	5.4	140/MWh (10am-9pm), $70/MWh (10pm-9am)
5	87,207,091	-22	≈0	$0.01M/MWh for battery cost
6	87,684,420	477,307	0.6	Max power buy and sales is 8, 7, and 4 MW in factory, warehouse and store, respectively
7	85,326,622	-1,880,491	-2.2	$1M/MW for PV, $0/MWh for selling price
8	89,927,218	2,720,105	3.1	$140/MWh for buying price in Reno
9	88578703	1371591	1.6	140/MWh (10am-9pm), $70/MWh (10pm-9am) in Reno

Table 10: Weekly Product Demand of the 4F-2W-4S Network

	Product A		Product B	
	Mean	Standard Deviation	Mean	Standard Deviation
Store 1	250	35	200	40
Store 2	350	42	300	57
Store 3	180	45	160	30
Store 4	220	40	190	40

Table 11: Microgrid Sizing of the 4F-2W-4S Network for the Benchmark Study (Case 1)

	Factory					Warehouse			Store			
	1	2	3	4		1	2		1	2	3	4
WT (MW)	0	0	0	0	WT	3.18	7.02	WT	4.28	0	0	18
PV (MW)	0	0	0	6.41	PV	7.09	0	PV	0	0	0	0
ESS (MWh)	0	0	0	0	ESS	0	0	ESS	0	0	0	0

Table A1: Resource Data for 2F-1W-2S Network (Note: F1=Factory 1, F2=Factory 2)

	Labor (hour)		Machine (hour)			Labor (hour)		Machine (hour)	
Week	F1	F2	F1	F2	Week	F1	F2	F1	F2
1	17871	19412	122693	150577	27	17567	19081	122998	150953
2	23963	26028	161238	197883	28	27251	29599	185471	227623
3	15531	16870	105179	129084	29	15008	16302	104506	128257
4	23810	25862	164141	201447	30	24055	26129	164533	201928
5	17020	18487	115050	141198	31	17082	18554	116094	142480
6	25516	27715	178157	218648	32	24361	26462	166074	203818
7	15806	17167	109757	134701	33	14922	16208	105226	129142
8	24907	27054	172894	212188	34	25848	28076	177572	217930
9	16817	18266	115034	141178	35	17068	18539	117494	144198
10	25744	27963	177118	217372	36	21218	23047	147419	180923
11	15654	17004	105661	129674	37	14681	15946	99626	122268
12	24750	26883	173807	213307	38	19834	21544	137372	168593
13	17130	18607	115341	141554	39	15590	16934	106354	130525
14	26236	28498	177504	217847	40	23474	25497	164676	202102
15	15336	16657	105793	129836	41	16581	18011	114349	140338
16	26527	28814	182681	224199	42	22794	24759	157022	192708
17	15736	17093	106150	130276	43	16545	17971	113408	139182
18	23364	25378	160770	197309	44	22714	24673	158422	194427
19	17637	15964	120826	148288	45	15986	17364	109791	134743
20	26231	28492	178312	218837	46	23443	25465	161554	198270
21	18956	20590	128436	157626	47	17212	18696	117720	144474
22	27107	29443	187268	229829	48	21403	23247	149436	183400
23	13394	14549	94626	116132	49	17975	19524	119144	146222
24	24284	26377	163848	201087	50	23839	25895	165547	203171
25	14600	15859	101396	124441	51	18728	16952	128554	157771
26	21334	23173	144616	177482	52	22326	24251	151885	186404

Table A2: Resource Data for 4F-2W-4S Network for Weeks 1-26

	Labor (hour)				Machine (hour)			
Week	Factory 1	Factory 2	Factory 3	Factory 4	Factory 1	Factory 2	Factory 3	Factory 4
1	8846	10812	8541	12812	60733	74229	66254	99381
2	11862	14497	11452	17178	79813	97549	87069	130603
3	7688	9396	7423	11134	52064	63633	56797	85195
4	11786	14405	11379	17069	81250	99305	88637	132955
5	8425	10297	8134	12202	56950	69605	62127	93191
6	12630	15437	12194	18292	88188	107785	96205	144308
7	7824	9562	7554	11330	54330	66403	59269	88903
8	12329	15069	11904	17856	85582	104601	93363	140044
9	8324	10174	8037	12056	56942	69596	62118	93177
10	12743	15575	12304	18456	87673	107156	95644	143465
11	7749	9471	7482	11223	52302	63925	57057	85585
12	12251	14974	11829	17743	86034	105153	93855	140783
13	8480	10364	8187	12281	57094	69781	62284	93426
14	12987	15873	12539	18808	87864	107390	95853	143779
15	7591	9278	7329	10994	52367	64005	57128	85692
16	13131	16049	12678	19018	90427	110522	98648	147971
17	7789	9520	7521	11281	52544	64221	57321	85982
18	11565	14135	11166	16750	79581	97266	86816	130224
19	8730	10670	7024	10536	59809	73100	65247	97870
20	12984	15870	12537	18805	88264	107879	96288	144432
21	9383	11468	9059	13589	63576	77704	69355	104033
22	13418	16400	12955	19432	92698	113297	101125	151687
23	6630	8104	6401	9602	46840	57249	51098	76647
24	12021	14692	11606	17409	81105	99128	88478	132717
25	7227	8833	6978	10467	50191	61345	54754	82131
26	10560	12907	10196	15294	71585	87492	78092	117138

Table A2: Resource Data for 4F-2W-4S Network for Weeks 27-52 (Continued)

	Labor (hour)				Machine (hour)			
Week	Factory 1	Factory 2	Factory 3	Factory 4	Factory 1	Factory 2	Factory 3	Factory 4
27	8696	10628	8396	12594	60884	74414	66419	99629
28	13489	16487	13024	19535	91808	112210	100154	150231
29	7429	9080	7173	10759	51731	63226	56433	84650
30	11907	14553	11497	17245	81444	99543	88848	133272
31	8455	10334	8164	12246	57467	70237	62691	94037
32	12059	14739	11643	17465	82207	100475	89680	134520
33	7386	9028	7132	10698	52087	63662	56822	85233
34	12795	15638	12354	18530	87898	107431	95889	143834
35	8449	10326	8157	12236	58160	71084	63447	95171
36	10503	12837	10141	15211	72972	89188	79606	119409
37	7267	8882	7016	10524	49315	60273	53798	80697
38	9818	11999	9479	14219	67999	83110	74181	111272
39	7717	9432	7451	11177	52645	64344	57431	86147
40	11620	14202	11219	16828	81515	99629	88925	133387
41	8207	10031	7925	11887	56603	69181	61749	92623
42	11283	13790	10894	16341	77726	94999	84792	127187
43	8190	10010	7907	11861	56137	68612	61240	91860
44	11243	13742	10856	16284	78419	95845	85548	128322
45	7913	9671	7640	11460	54347	66424	59287	88931
46	11604	14183	11204	16807	79969	97740	87239	130858
47	8520	10413	8226	12339	58271	71221	63569	95353
48	10595	12949	10229	15343	73971	90409	80696	121044
49	8898	10875	8591	12886	58976	72082	64338	96507
50	11800	14423	11394	17091	81946	100156	89395	134093
51	9270	11330	7459	11189	63634	77775	69419	104129
52	11051	13507	10671	16006	75183	91891	82018	123027

1.

Manuscript Title:

Supply Chain Design for Transactive Energy Operations in the Nexus of Manufacturing, Microgrid and Climate

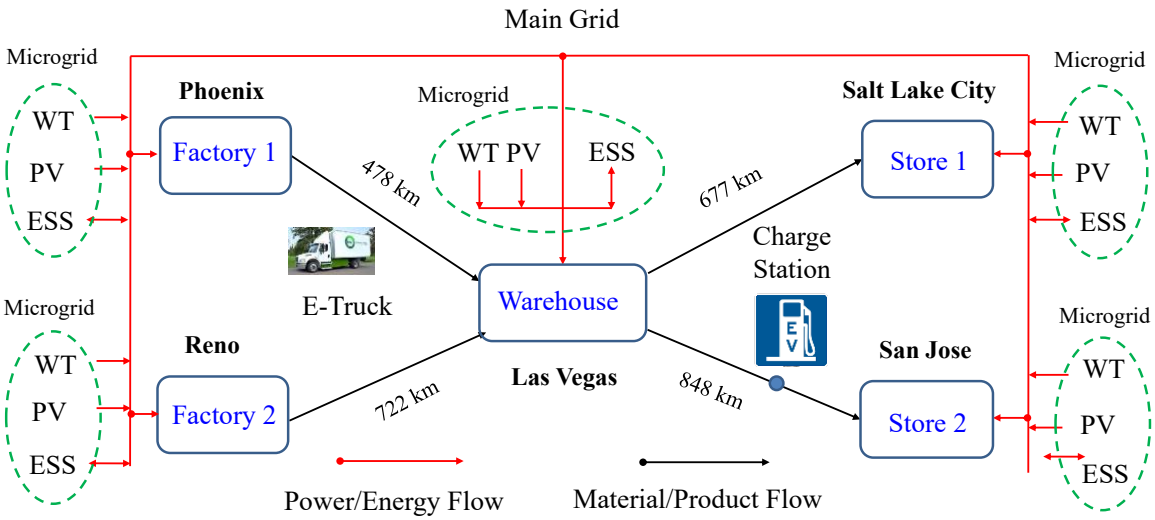


Figure 1: A Three-Tire Supply Chain Network with Microgrid Integration

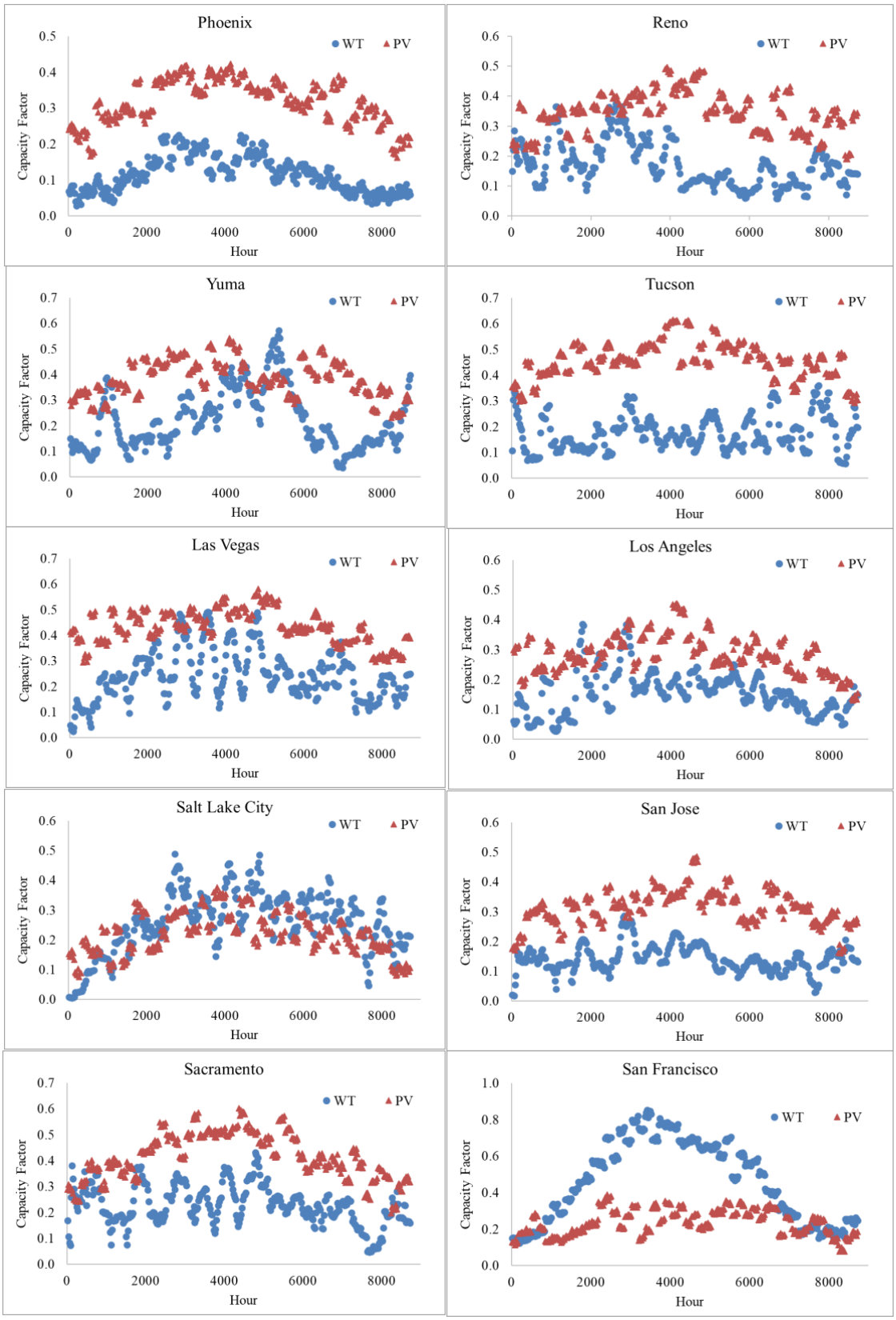


Figure 2: Hourly Capacity Factor of WT and PV from January to December

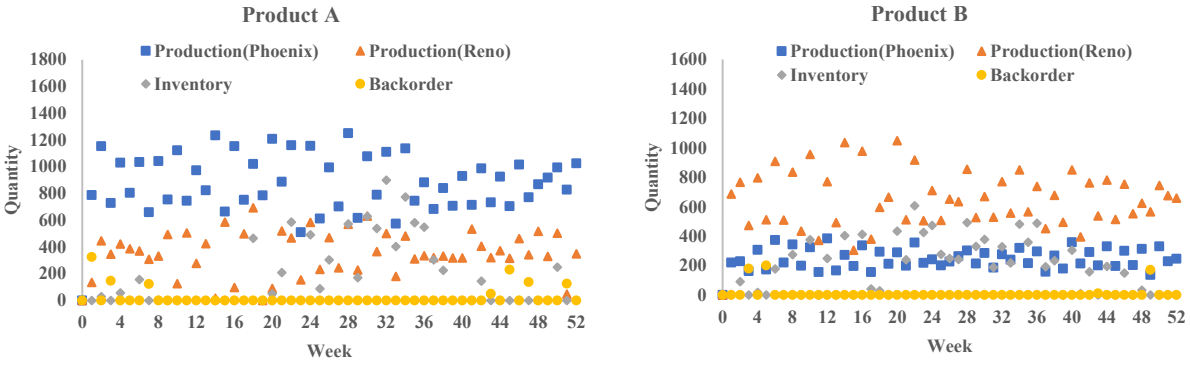


Figure 3: Production and Inventory Decision of the 2F-1W-2S Network

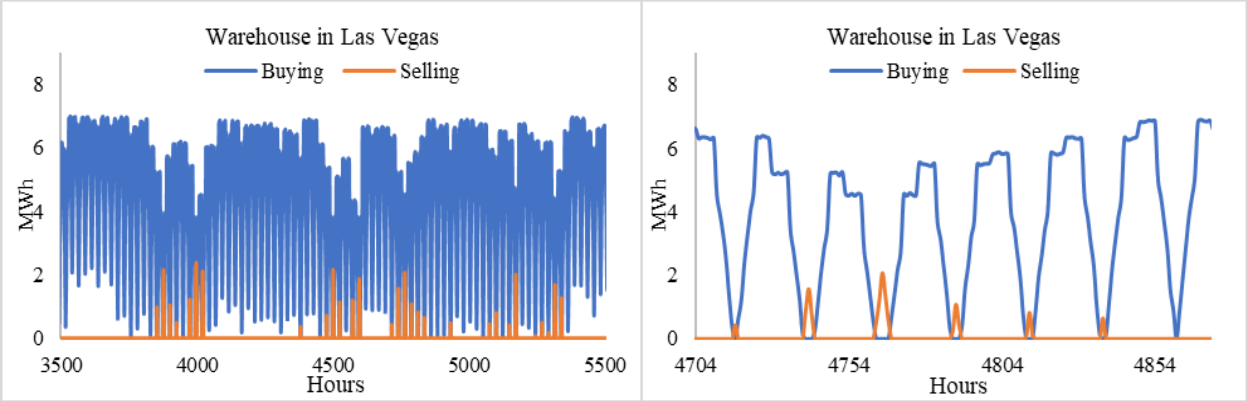


Figure 4: Prosumer Energy Trading in Las Vegas Warehouse

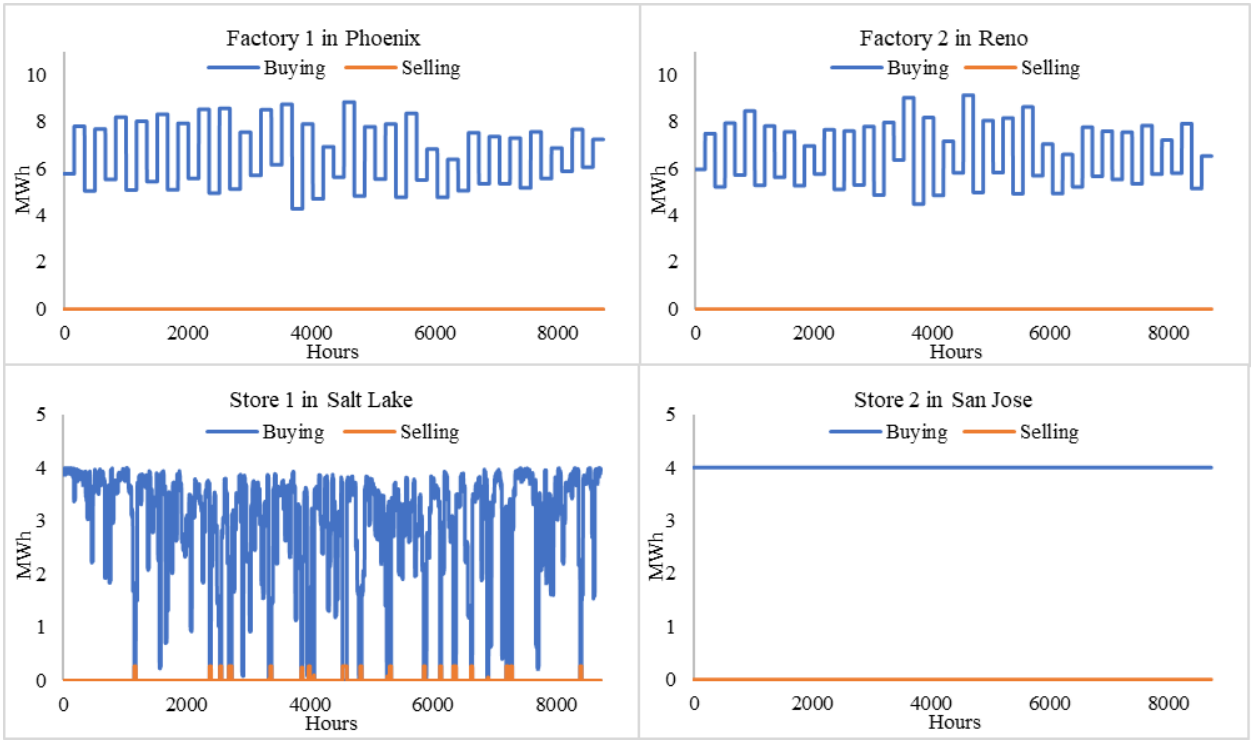


Figure 5: Hourly Energy Transactions in Factories and Stores

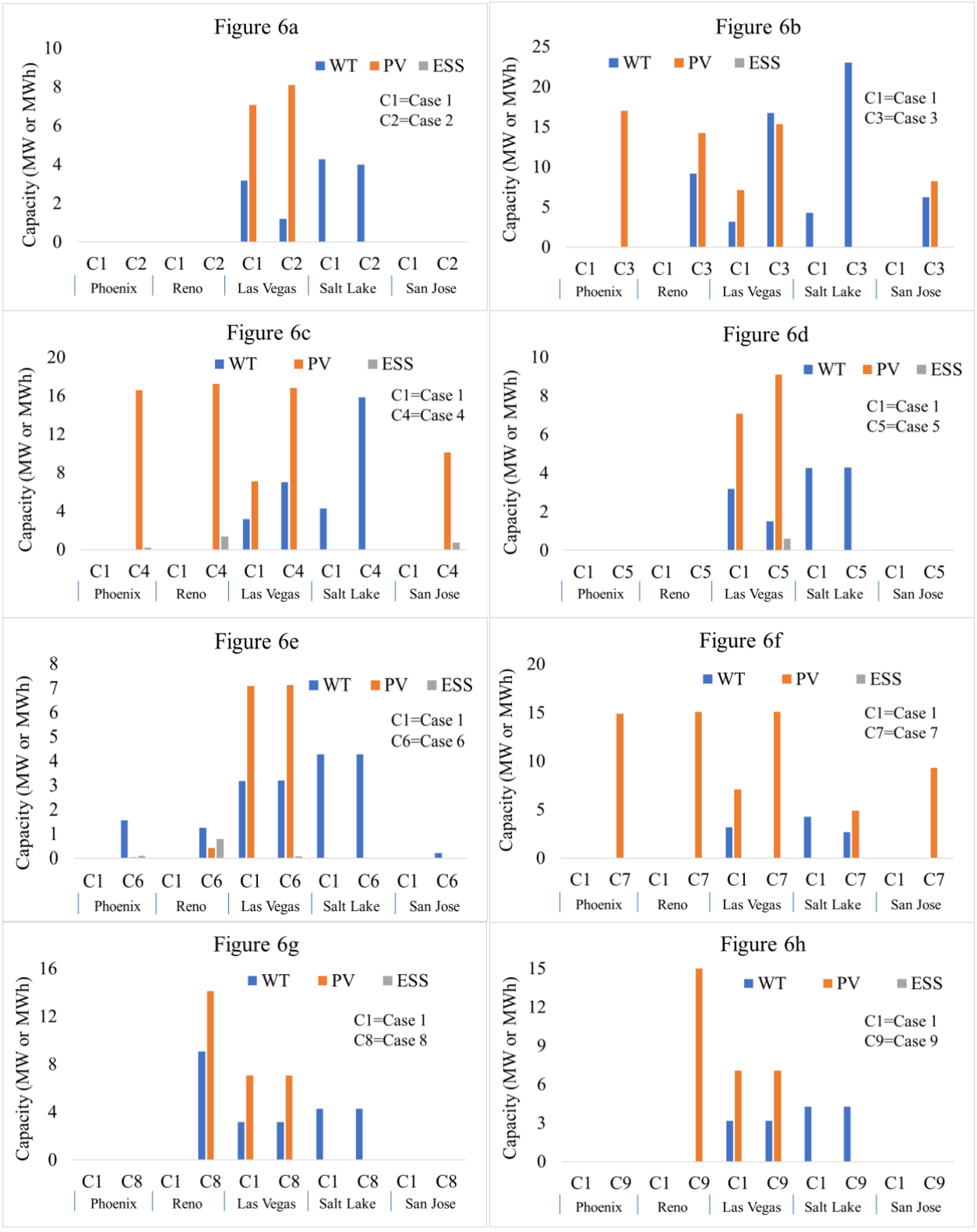


Figure 6: Microgrid Sizing for Cases 2 to 9

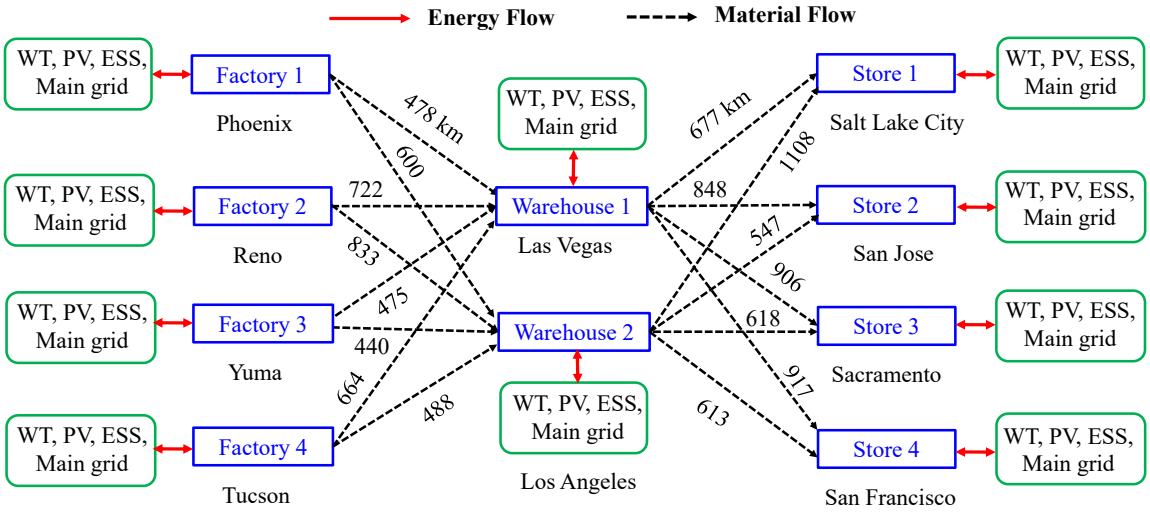


Figure 7: A 4-Factory, 2-Warehouse and 4-Store Supply Chain

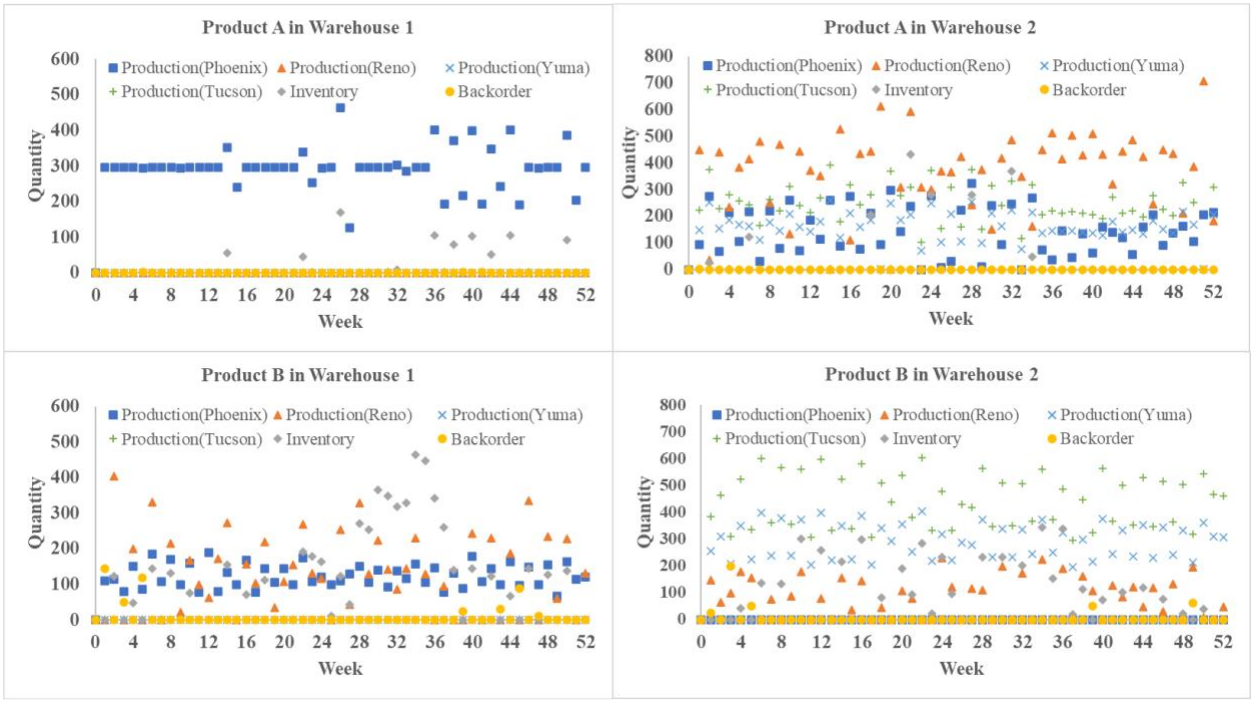


Figure 8: Production and Inventory Planning for the 4F-2W-4S Network